Fermi-surface geometry of the Cu−27.5 at. % Pd disordered alloy and short-range order

I. Matsumoto
Department of Synchrotron Radiation Science, The Graduate University for Advanced Studies, Tsukuba, Ibaraki 305-0801, Japan

H. Kawata
Photon Factory, High Energy Accelerator Research Organization, Tsukuba, Ibaraki 305-0801, Japan

N. Shiotani
Tokyo University of Fisheries, Kounan, Minato, Tokyo 108-8477, Japan
(Received 8 June 2001; published 29 October 2001)

The Fermi surface of the disordered phase of Cu-27.5 at. % Pd alloy is three-dimensionally mapped out from high-resolution Compton scattering data. In reference to the well-known Fermi surface of pure Cu, the neck disappears and the belly becomes flattened in the [110] direction in the alloy forming a set of parallel sheets. The obtained [110] Fermi radius is in good accord with the value indirectly determined from the separation along the [110] direction between the x-ray diffuse scattering peaks. The results are regarded as the experimental evidences to support the previous theoretical predictions that the pair of the parallel sheets of the Fermi surface drives the short-range order in this disordered phase.

DOI: 10.1103/PhysRevB.64.195132 PACS number(s): 71.18.+y, 71.23.−k

I. INTRODUCTION

Several theoretical and experimental studies have found that the geometry of the Fermi surface drives a variety of ordering phenomena such as magnetic ordering in the rare earths and their alloys,[1–3] compositional ordering in binary alloys,[4–6] and magneto-oscillatory coupling in magnetic multilayers separated by nonmagnetic spacer layers.[7] The theory indicates that the ordering is governed by the nesting of specific sheets of the Fermi surface in the disordered states. Nesting describes the coincidence of two approximately parallel Fermi surface sheets when translated by some distance in $\mathbf{k}$ space. In the presence of nesting the disordered phase becomes unstable to an ordering modulation whose period is inversely proportional to the relevant nesting vector. Regarding the compositional ordering in binary alloys, the Cu-Pd system is a traditional touchstone and has been the subject of extensive investigations because the system exhibits a large variety of ordered phases and short-range order in the disordered phase.[8] Of special interest and immediate relevance to the present subject is the short-range order which is directly observable as diffuse scattering peaks in the x-ray, neutron, and electron diffraction.[9] The previous explanation of the diffuse scattering peaks is based on the Clapp-Moss formula[4,5] for the short-range order parameter $\alpha(\mathbf{k})=[1+2m_Am_B\beta W(\mathbf{k})]^{-1}$, where $W(\mathbf{k})$ is the lattice Fourier transform of a pair-wise interchange potential, m_A and m_B are the fraction of A and B atoms in the alloy, and $\beta=(k_BT)^{-1}$, where k_B is the Boltzmann constant and T is the temperature. The diffuse scattering intensity $I(\mathbf{k})$ is proportional to $\alpha(\mathbf{k})$. The suggestion of Moss[10] is that $W(\mathbf{k})$ can be calculated in perturbation theory to second order in the electron-ion potential and hence is proportional to the one-electron susceptibility $\chi_0(\mathbf{k})$ which can peak at $\mathbf{k}_0$'s that connect parallel flat segments of the Fermi surface leading to peaks in $\alpha(\mathbf{k})$ and $I(\mathbf{k})$ at $\mathbf{k}_0$. Then, the separation m along the [110] direction between the diffuse scattering peaks is related to the Fermi radius in the [110] direction, $k_F[110]$, as

$$m=\sqrt{2}-4k_F[110], \tag{1}$$

where both m and $k_F[110]$ are measured in units of $4\pi/a$ and a is the lattice constant. Later, Gyorffy and Stocks[6] presented an alternative theory which was free from the assumption of pair potentials and second-order perturbation theory. They adapted the density-functional approach for classical liquids to a lattice-gas model of alloy configurations. The theory concludes, in accord with the suggestion of Moss, that when there are well defined bands and well defined flat sheets of the Fermi surface, the diffuse scattering intensity will peak at $\mathbf{k}_0$'s which connect these flat sheets. Using the KKR-CPA scheme, they calculated the Fermi surface on the ΓXWK plane in the first Brillouin zone for Cu_xPd_{1-x} ($x=0.9$, 0.75 and 0.6) and showed the increasing flattening of the Fermi surface in the [110] direction with increasing Pd content. The diffuse scattering in the Cu-Pd system was studied extensively by Ohshima and Watanabe.[11] The $k_F[110]$ of Cu_xPd_{1-x} ($x=0.9$, 0.75 and 0.6) obtained by Gyorffy and Stocks are right on the curve of m vs Pd concentration measured by Ohshima and Watanabe when the $k_F[110]$'s are converted to m by Eq. (1).

Direct experimental studies of the radii of the Fermi surface of the Cu-Pd alloys were reported by Hasegawa *et al.*[12] using positron annihilation with crossed- and long-slit geometry, and by Smedskjaer *et al.*[13] using the same method but with 2D-ACAR geometry. The latter accompanied the results of the KKR-CPA calculations which were in excellent agreement with the experimental results. When the Fermi surface radius k_F in a given direction was normalized by the Brillouin-zone dimension k_{BZ} along the same direction, it was found experimentally as well as theoretically that both [100] and [110] radii decreased almost linearly with Pd concentration. However, the two experimental results differ in that the slope for the [100] radius of Ref. 12 is a little gentler

than that of Ref. 13, and that for the [110] radius of Ref. 13 is much steeper than that of Ref. 12. Smedskjaer *et al*. have concluded that the more rapid decrease of k_F/k_{BZ} with Pd concentration in the [110] direction compared with that in the [100] direction indicates a flattening of the Fermi surface in the vicinity of [110] upon addition of Pd. However, both experimental and theoretical results gave the radii of only two directions and do not show how far the flattening extends in the directions perpendicular to the [110] directions. In addition, it is noted that there is a discrepancy on the [100] radius between the two theories. Reference 6 gives a larger value by about 6% than Ref. 13 at 25 at.% Pd. Further, disappearance of the neck in the alloys of Pd concentration above 20 at.% was inconclusive in Ref. 12. The issue is, therefore, to settle the discrepancy between two experimental results and to evaluate the two theoretical results by obtaining new direct experimental information about the three-dimensional geometry of the Fermi surface of the alloys.

The aims of this paper are to present the Fermi surfaces of Cu-27.5 at.% Pd in the disordered phase and pure Cu as the reference obtained by Compton scattering, and to show three dimensionally that the Fermi surface of the alloy is indeed flattened in the Γ-K direction.

In a Compton scattering experiment one measures the so-called Compton profile,[14]

$$J(p_z)=\int\int \rho(\mathbf{p})dp_x dp_y, \tag{2}$$

where p_z is taken along the x-ray scattering vector and

$$\rho(\mathbf{p})=(2\pi)^{-3}\sum_i \left|\int \psi_i(\mathbf{r})\exp(-i\mathbf{p}\cdot\mathbf{r})d\mathbf{r}\right|^2 \tag{3}$$

is the ground-state momentum density of the electron system, expressed in terms of the electron wave functions ψ. The summation in Eq. (3) extends over the occupied states. Thus the Compton profile contains signatures of the Fermi surface breaks in the underlying three dimensional (3D) momentum density $\rho(\mathbf{p})$. Unlike traditional spectroscopies for studying Fermiology, Compton scattering is not sensitive to structural disorders, which makes this technique particularly suitable for investigating electronic structure of disordered alloys. One disadvantage easily seen in Eq. (2) is that the profile is a twice integrated quantity of the 3D $\rho(\mathbf{p})$ and thus the Fermi surface breaks may not be well resolved. This disadvantage, however, can be overcome by reconstructing $\rho(\mathbf{p})$ from the profiles measured along a series of directions. The method first used to reconstruct $\rho(\mathbf{p})$ from Compton profiles or one-dimensional positron annihilation angular correlation spectra was formulated by Mijnarends[15] who, in the vein of Cormack's approach,[16] expanded both $\rho(\mathbf{p})$ and the measured profiles into lattice harmonics and derived a relation between the two expansions. Another way to obtain $\rho(\mathbf{p})$ is to utilize the properties of the so-called reciprocal form factor

$$B(\mathbf{r})=\int \rho(\mathbf{p})\exp(-i\mathbf{p}\cdot\mathbf{r})d\mathbf{p}. \tag{4}$$

From Eqs. (2) and (4) we get

$$B(0,0,z)=\int J(p_z)\exp(-ip_z z)dp_z. \tag{5}$$

When $J(p_z)$ for p_z set along many different crystalline axes are measured, the values of $B(\mathbf{r})$ can be obtained on the lines in real space which are parallel to p_z. From there onward we can follow two different approaches to obtain $B(\mathbf{r})$ in all of $\mathbf{r}$: Either we expand $B(\mathbf{r})$ into a set of appropriately chosen basis function as proposed by Hansen[17] and applied to Li by Schülke *et al.*[18] and to Li-Mg disordered alloys by Stutz *et al.*,[19] or we straightforwardly map $B(\mathbf{r})$ in $\mathbf{r}$ space by interpolation. The latter method is called the direct Fourier transform method. Once $B(\mathbf{r})$ is known, the inverse Fourier transform can be carried out to obtain $\rho(\mathbf{p})$. The direct Fourier transform method was first applied to reconstruct the 3D electron-positron momentum density from the 2D angular correlation of positron annihilation radiation measured by Suzuki *et al.*[20] on Ti and Zr. Later, the method was applied to reconstruct the 3D spin-dependent momentum density from magnetic Compton profiles of Fe by Tanaka *et al.*[21] Recently the method was also applied to a study of the Fermi surface of Li by Tanaka *et al.*[22] Some words for other reconstruction methods are appropriate. Cormack's method was developed further by Kontrym-Sznajd *et al.*,[23] and applied by Dugdale *et al.*[24] to the reconstruction of the 2D electron momentum density of Cr from several directional Compton profiles. The essential of Cormack's method is the expansion of both Compton profiles and momentum density into polar Fourier series. Lastly, the maximum entropy method, which is already an established method in the field of charge-density reconstruction, was adapted to momentum density reconstruction by Dobrzynski and Holas.[25] In this study we employ the direct Fourier transform method because the method makes no implicit functional assumptions concerning the shape of $\rho(\mathbf{p})$.

II. EXPERIMENT

Single crystals of Cu-27.5 at.% Pd with surface normals oriented along the [100], [110], and [111] directions were used. The disordered phase was secured by quenching the specimen into iced water after annealing at 600 °C for ten days. The Compton profiles have been measured at the PF-AR NE1A1 beamline of the KEK, where for the incident beam 60 keV x-rays are available with a rate of 1.5×10^{13} photons/s. The Compton spectrometer[26] is unique in design and consists of four independent analyzing systems arranged on the surface of a cone that provides a scattering angle of 160° to all of the analyzing system. Each analyzing system is equipped with a triangular Cauchois-type Si (422) crystal analyzer bent to a radius of 2.5 m and an image plate as a position sensitive detector. The reader is referred to Sakurai *et al.*[26] for the details of the spectrometer. Two of the analyzing systems are used for the present measurements, one in the horizontal and the other in the vertical position viewed from the base of the cone, to obtain 28 directional profiles. The directions along which the Compton profiles were measured are shown in Fig. 1 using the irreducible orientation

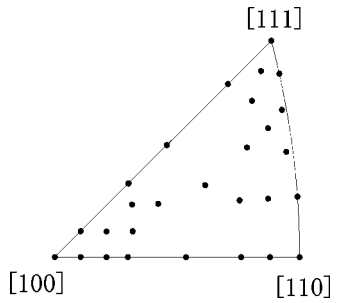

FIG. 1. The directions along which the Compton profiles of both pure Cu and Cu-27.5 at. % Pd alloy are measured are represented by the full circles in the irreducible orientation triangle of cubic symmetry.

triangle. The directions were so chosen that the neck at L and the [110] radius of the belly could be determined as precisely as possible. As the reference, the profiles of pure Cu were also measured along the same directions as those of the alloy. The overall instrumental resolution was 0.13 atomic units (a.u.) in full width at half maximum (FWHM). The total accumulated counts under each profile was about 1.2×10^8. The measured profiles were corrected for the necessary energy dependent corrections such as absorption, detector and analyzer efficiency, and scattering cross section. The contribution of double scattering was estimated by a Monte Carlo simulation programmed by Sakai.[27] The ratio of the total intensity of double scattering to that of single scattering turned out to be 0.035.

The standard deviations (error bars) were evaluated as follows. The data stored in the image plate contain errors originating in the photon counting process, in addition to errors introduced by the read-out system. The latter errors depend mainly on the stability of the laser and the uniformity of the photostimulable phosphor in the image plate, and has been estimated to be about 0.5% of N_0 counts by Ito and Amemiya.[28] The total standard deviation σ for N_0 counts, a typical of which at the Compton peak is about 6×10^5, is given by

$$\sigma=\sqrt{N_0}+0.005\times N_0. \tag{6}$$

The method of calculation of error propagation is the same as that Tanaka *et al.*[22] developed.

The diffuse scattering peaks around the (330) Bragg spot have been measured using a conventional four circle diffractometer. The separation m along the [110] direction between the diffuse scattering peaks is 0.108 ± 0.0017 in units of the distance between the (000) and (002), that is $4\pi/a$, where a is the measured lattice constant. The present value is right on the curve of m vs Pd concentration obtained by Ohshima and Watanabe.[11]

III. RECONSTRUCTION

The valence electron profile is obtained by subtracting from the corrected profile the core electron contributions which are assumed to be given by the weighted sum of theoretical profiles of electrons from $(1s)^2$ to $(3p)^6$ of Cu atom and from $(1s)^2$ to $(4p)^6$ of Pd atom calculated by Biggs *et al.*[29] Each valence electron profile was Fourier transformed to a B function. Inevitably the B function had some high frequency components due to the statistical errors and noises produced in the process of reading out the image plate. To reduce unwanted high frequency components, a filtering function has to be applied. We examined various types of filtering function in the test reconstruction of the 3D stepwise free electron momentum density with a cutoff at 0.76 a.u., which corresponds to the average radius of pure Cu Fermi surface, by assigning one parabolic profile to twenty different directions. The following filtering function was found best to reproduce the stepwise momentum density without introducing ripples at the cutoff.

$$B^{\text{filterd}}(i\Delta z)=B(i\Delta z)(N-i)/N, \tag{7}$$

where N represents the total number of points on z axis and Δz is the distance between two points. However, applying the function inevitably introduces an extra resolution of 0.02 a.u. (FWHM). Hence the overall momentum resolution due to the instrumental resolution and the filtering becomes 0.145 a.u. (FWHM). For interpolation the following scheme is used. The value of B at an arbitrary $\mathbf{r}$ is given as

$$B(\mathbf{r})=A[a^{-1}B_i(\mathbf{r}_1)+b^{-1}B_j(\mathbf{r}_2)+c^{-1}B_k(\mathbf{r}_3)]. \tag{8}$$

Here, $r=r_1=r_2=r_3$, and $B_i(\mathbf{r}_1)$, $B_j(\mathbf{r}_2)$, and $B_k(\mathbf{r}_3)$ are three B's whose directions are closest to and enclose the direction $\mathbf{r}$, and a, (b and c) is the distance between $\mathbf{r}$ and $\mathbf{r}_1$ ($\mathbf{r}_2$, $\mathbf{r}_3$) on the sphere of radius $\mathbf{r}$, and A is the normalization constant. This interpolation method was also tested in a way that one parabolic profile was assigned to 15 different directions, then checking was done whether or not the same profile could be reproduced for any arbitrary direction.

IV. RESULTS AND DISCUSSION

Figure 2 shows the contour map of the reconstructed momentum density of the alloy in the (100) plane together with the corresponding error map. The largest error, 2%, is found at $p=0$. In this reconstruction method the high frequency noises in the measured profiles, in other words fluctuations of B in large $\mathbf{r}$, inevitably accumulate at the origin of the reconstructed momentum density because of back Fourier transform. A strong anisotropic error distribution is seen. The large errors are found on the [100] axis and its vicinity and they change little with p in the range of interest. Also along the [110] direction some accumulation of errors are found. This anisotropic error distribution is similar to that found by Tanaka *et al.*[22] who employed the same reconstruction method, but with different filtering and interpolation schemes from the present ones, to obtain the 3D momentum density in Li. Their explanation for the anisotropic distribution of errors is also true for the present error distribution.

It is noted that the momentum density contour lines are

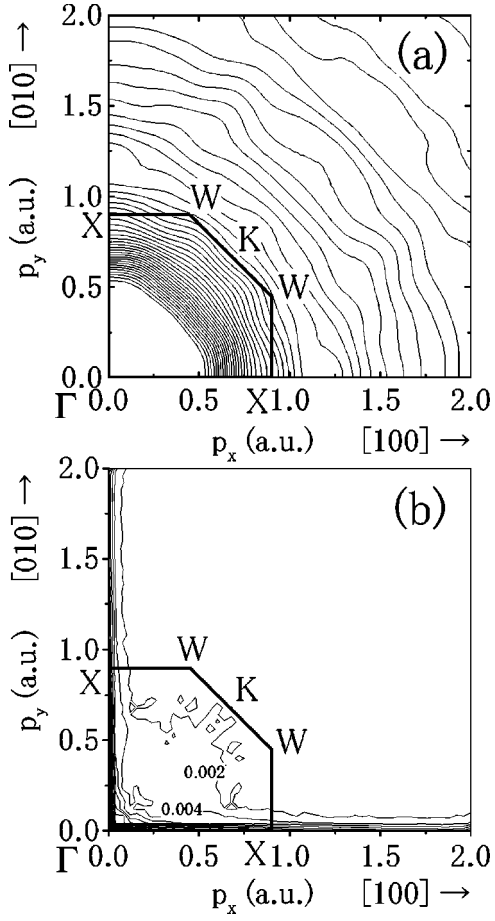

FIG. 2. (a) The contour map of the reconstructed momentum density of Cu-27.5 at. % Pd disordered phase on the (100) plane. The contour interval is 0.25 electrons/a.u.^{3} (b) The corresponding error map. The contour step is 0.002 electrons/a.u.^{3}

flattened in the Γ-K direction. In order to find the breaks at the Fermi momenta in the reconstructed momentum density, first we examined the effects of the resolution on the position of the breaks in the theoretical $\rho(\mathbf{p})$ in pure Cu given by Kubo *et al.*[30] by three-dimensionally convoluting $\rho(\mathbf{p})$ with the present overall resolution. We have found that a position of a peak in $d\rho^{\mathrm{conv}}(\mathbf{p})/d\mathbf{p}$, $\mathbf{p}$ on the [100] axis, is shifted by -0.02 a.u. from the position of the stepwise break in $\rho(\mathbf{p})$, while $\mathbf{p}$ on the [110] axis is not shifted. The amount of shift depends on how stationary $\rho(\mathbf{p})$ at the Fermi momenta is in directions perpendicular to the radial direction. Even though we know this fact, since we do not have theoretical $\rho(\mathbf{p})$ in the alloy to estimate the amount of shift for various directions, we use the position of a peak in the first derivatives of the reconstructed momentum density as the position of the break at the Fermi momentum. Figure 3 shows the momentum density of the alloy on the Γ-X axis and its first derivatives. There are noticeable ripples in high momenta (>1.5 a.u.), the appearance of which is an inevitable artifact of Fourier transform of discretely sampled data. The origin of these ripples is a combination of the so-called aliasing[31] and the Gibbs phenomenon.[32] We have applied a slight convolution smoothing, not to a degree that the resolution gets worsened, to the Compton profiles to suppress

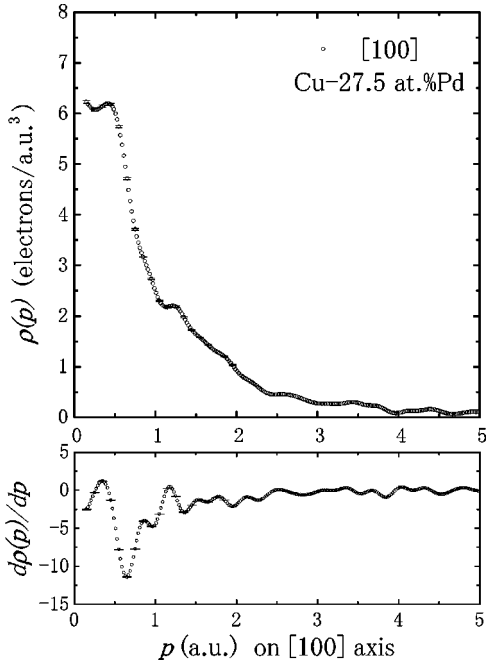

FIG. 3. Momentum density $\rho(p)$ of Cu-27.5 at. % Pd (upper frame) and its first derivatives (lower frame) on the [100] axis.

these ripples and to put them away from the Fermi momenta. Thus, our method to determine the Fermi momenta is not affected by these artifacts. It is noted that a bump just beyond 1 a.u. in the momentum density is due to the the first higher momentum component (the corresponding bump in the theoretical density of pure Cu is seen in Fig. 4 of Ref. 30). The Fermi momenta thus determined in the (100) and (110) planes are shown in Fig. 4. The radii are normalized by the Brillouin-zone dimension. It is clearly seen that the Fermi surface of the alloy gets flattened in the [110] direction forming a set of parallel sheets, and has no neck at L. In comparison with the theoretical Fermi surface of Cu-25 at. % Pd of Ref. 6 the flattening is not so much extended in the direction perpendicular to the [110] direction and the Fermi surface is more rounded in the [100] direction in the present Cu-27.5 at. % Pd alloy. Considering the small difference in Pd content, we may say that the theory overestimated the extent of the flattening, which resulted in giving the larger k_F in the [100] direction than any of the experimental value (see Fig. 5). In the present study the k_F in the [110] direction is 0.59 ± 0.01 a.u. in the alloy while 0.69 ± 0.01 a.u. in pure Cu. The k_F in the [100] direction is 0.66 ± 0.01 a.u. in the alloy and 0.74 ± 0.01 a.u. in pure Cu.

Although a few band structure computations of the Cu-Pd system[33–35] have been reported focusing on the density of states and x-ray photoelectron spectroscopy spectra, there is no calculation of the complete geometry of the Fermi surface of Cu-27.5 at. % Pd alloy which is directly compared with the present result. However, Fig. 1 of Ref. 13 which includes the results of Refs. 6 and 12 serves the purpose and is reproduced in Fig. 4 together with the present results. The present [100] and [110] radii of pure Cu are in good agreement with all of the previous results. The present [110] radius of the

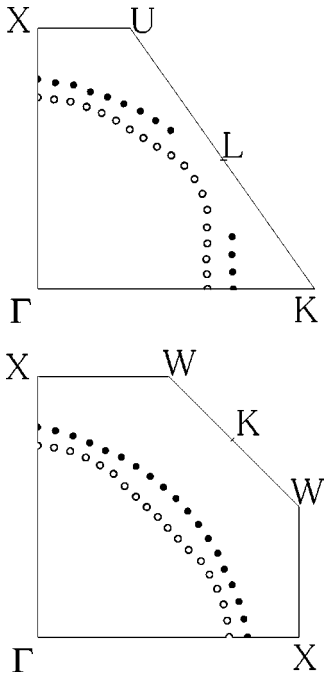

FIG. 4. The Fermi radii of pure Cu (full circles) and Cu-27.5 at. % Pd (open circles) in the disordered phase on the ΓXULK plane (upper) and the ΓXWK plane (lower). They are normalized by the the Brillouin-zone dimension. The size of the circles is that of the error involved in the radial direction.

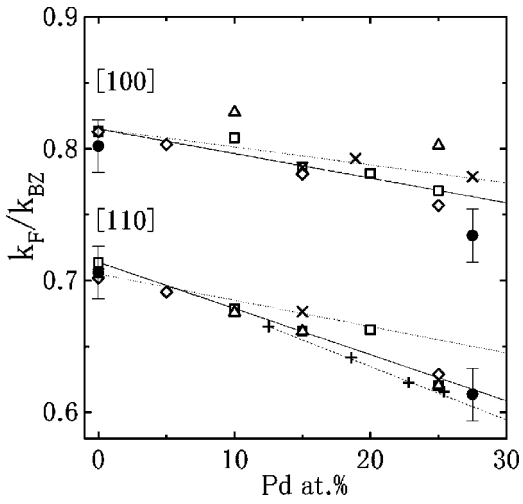

FIG. 5. k_F/k_{BZ}, where k_F is the Fermi surface radius in a given direction and k_{BZ} is the Brillouin-zone dimension along the same direction, as a function of Pd concentration. The full circles represent the present results. The following is reproduced from Fig. 1 of Ref. 13. The squares and the solid lines represent the experimental results of Smedskjaer *et al.* (Ref. 13). The lozenges represent theoretical results of Rao *et al.* (Ref. 34) and Smedskjaer *et al.* The triangles represents the theoretical results of Gyorffy and Stocks (Ref. 6). The dotted line represents the least-squares linear fits to the data (crosses) of Hasegawa *et al.* (Ref. 12). The plusses and dashed line represent the results of Ohshima and Watanabe (Ref. 11).

alloy is on the line given by Ref. 13. However, the [100] radius of the alloy is slightly smaller than that extrapolated by any of the previous experimental results. The discrepancy may be due to the above-mentioned effect of the resolution. Finally, putting the observed value of m in Eq. (1), we get 0.586 ± 0.001 a.u. for k_F in the [110] direction, which is in excellent agreement with the value of 0.59 a.u. determined from the break in the momentum density. The proposed relation between m and k_F holds very well at the present composition.

V. SUMMARY

We have measured the Compton profiles of Cu-27.5 at. % Pd in the disordered phase along 28 different directions, and those of Cu as the reference along the same directions. From them the three-dimensional electron momentum density has been reconstructed via the direct Fourier transform method. The Fermi momenta have been obtained from the positions of the peak in the first derivatives of the reconstructed momentum density. The Fermi surfaces of pure Cu and the alloy on the (100) and (110) planes have been mapped out to show that the Fermi surface of the alloy is flattened in the [110] direction forming a set of parallel sheets and has no neck at L. The [110] radius of the alloy is in good accord with the value extrapolated from previous experimental and theoretical results. However, the [100] radius of the alloy is slightly smaller than the value extrapolated from the previous experimental and theoretical results. In addition, the diffuse scattering peaks around the (330) Bragg spot have been measured. The separation m along the [110] direction between the diffuse scattering peaks has yielded the [110] radius which is in excellent agreement with the value obtained from the momentum density. All of these results are regarded as the experimental evidences to support previous theories that the pair of the parallel flat sheets of the Fermi surface drives the short-range order in this alloy. They also have demonstrated the capability of the Compton scattering to investigate Fermiology of concentrated disordered alloys.

ACKNOWLEDGMENTS

The authors are very grateful to H. M. Fretwell, S. B. Dugdale and M. A. Alam for stimulating discussion at the very early stage of this study. They are indebted to M. Hasegawa for letting them use his single crystals of Cu-27.5 at. % Pd. They would like to thank K. Ohshima for his very helpful discussion and preparation of the specimens in the disordered phase, and Y. Kubo for sending us the theoretical 3D momentum density in Cu. They would like to express their thanks to Y. Sato, H. Adachi, and H. Hashimoto for their help during the measurements. The measurements of the Compton profiles were carried out with the approval of the Photon Factory Advisory Committee, Proposal No. 97-G288 and 99-G144. This research is partially supported by Grant-in-Aid for Scientific Research No. 10440038, the Ministry of Education, Culture, Sports, Science and Technology, Japan.

[1] T. Kasuya, in *Magnetizm*, edited by G. T. Rado and H. Suhl (Academic, New York, 1966), Vol. IIB, p. 215.
[2] H. M. Fretwell, S. B. Dugdale, M. A. Alam, D. C. R. Hedley, A. Rodriguez-Gonzalez, and S. B. Palmer, Phys. Rev. Lett. **82**, 3867 (1999).
[3] S. B. Dugdale, H. M. Fretwell, M. A. Alam, G. Kontrym-Sznajd, R. N. West, and S. Badrzadeh, Phys. Rev. Lett. **79**, 941 (1997).
[4] P. C. Clapp and S. C. Moss, Phys. Rev. **142**, 418 (1966).
[5] P. C. Clapp and S. C. Moss, Phys. Rev. **171**, 754 (1968).
[6] B. L. Gyorffy and G. M. Stocks, Phys. Rev. Lett. **50**, 374 (1983).
[7] S. S. Parkin, Phys. Rev. Lett. **67**, 3598 (1991).
[8] See, for example, *Binary Alloy Phase Diagrams*, edited by T. B. Massalski (ASM International, 1990).
[9] M. A. Krivoglaz, *Theory of X-Ray and Thermal Neutron Scattering by Real Crystals* (Plenum, New York, 1969).
[10] S. C. Moss, Phys. Rev. Lett. **22**, 1108 (1969).
[11] K. Ohshima and D. Watanabe, Acta Crystallogr., Sect. A: Cryst. Phys., Diffr., Theor. Gen. Crystallogr. **29**, 520 (1973).
[12] M. Hasegawa, T. Suzuki, and M. Hirabayashi, J. Phys. Soc. Jpn. **43**, 89 (1977).
[13] L. C. Smedskjaer, R. Benedek, R. W. Siegel, D. G. Legnini, M. D. Stahulak, and A. Bansil, Phys. Rev. Lett. **59**, 2479 (1987).
[14] M. J. Cooper, Rep. Prog. Phys. **48**, 415 (1985).
[15] P. E. Mijnarends, Phys. Rev. **160**, 512 (1967); **178**, 622 (1969).
[16] A. M. Cormack, J. Appl. Phys. **34**, 2722 (1963).
[17] N. K. Hansen, *Reconstruction of the EMD from a Set of Directional Profiles* (Hahn Meitner Institute, Berlin, 1980), Rep. HMI B 342.
[18] W. Schülke, G. Stutz, F. Wohlert, and A. Kaprolat, Phys. Rev. B **54**, 14 381 (1996).
[19] G. Stutz, F. Wohlert, A. Kaprolat, W. Schülke, Y. Sakurai, Y. Tanaka, M. Ito, H. Kawata, N. Shiotani, S. Kaprzyk, and A. Bansil, Phys. Rev. B **60**, 7099 (1999).
[20] R. Suzuki, S. Tanigawa, N. Shiotani, M. Matsumoto, and S. Wakoh, J. Phys. Soc. Jpn. **58**, 3251 (1989).
[21] Y. Tanaka, N. Sakai, Y. Kubo, and H. Kawata, Phys. Rev. Lett. **70**, 1537 (1993).
[22] Y. Tanaka, Y. Sakurai, A. T. Stewart, N. Shiotani, P. E. Mijnarends, S. Kaprzyk, and A. Bansil, Phys. Rev. B **63**, 045120 (2001).
[23] G. Kontrym-Sznajd, R. N. West, and S. B. Dugdale, Mater. Sci. Forum **255-257**, 796 (1997).
[24] S. B. Dugdale, H. M. Fretwell, K. J. Chen, Y. Tanaka, A. Shukla, T. Buslaps, Ch. Bellin, G. Loupias, M. A. Alam, A. A. Manuel, P. Suortti, and N. Shiotani, J. Phys. Chem. Solids **61**, 361 (2000).
[25] L. Dobrzynski and A. Holas, Nucl. Instrum. Methods Phys. Res. A **383**, 589 (1996).
[26] Y. Sakurai, M. Ito, T. Urai, Y. Tanaka, N. Sakai, T. Iwazumi, H. Kawata, M. Ando, and N. Shiotani, Rev. Sci. Instrum. **63**, 1190 (1992).
[27] N. Sakai, J. Phys. Soc. Jpn. **56**, 2477 (1987).
[28] M. Ito and Y. Amemiya, Nucl. Instrum. Methods Phys. Res. A **310**, 369 (1991).
[29] F. Biggs, L. B. Mendelsohn, and J. B. Mann, At. Data Nucl. Data Tables **16**, 201 (1975).
[30] Y. Kubo, Y. Sakurai, and N. Shiotani, J. Phys.: Condens. Matter **11**, 1683 (1999).
[31] W. H. Press, B. P. Flannery, S. A. Teukolsky, and W. T. Vetterling, *Numerical Recipes in C* (Cambridge University Press, Cambridge, 1988).
[32] T. W. Körner, *Fourier Analysis* (Cambridge University Press, Cambridge, 1988).
[33] R. S. Rao, A. Bansil, H. Asonen, and M. Pessa, Phys. Rev. B **29**, 1713 (1984).
[34] H. Winter, P. J. Durham, W. M. Temmerman, and G. M. Stocks, Phys. Rev. B **33**, 2370 (1986).
[35] S. K. Bose, J. Kudrnovsky, O. Jepsen, and O. K. Andersen, Phys. Rev. B **45**, 8272 (1992).